VO_2 oscillators coupling for Neuromorphic Computation

Elisabetta Corti[1,2], Bernd Gotsmann[1], Kirsten Moselund[1], Igor Stolichnov[2], Adrian Ionescu[2], Guofang Zhong[3], John Robertson[3] and Siegfried Karg[1]

[1] IBM Research – Zurich, Rüschlikon, Switzerland

[2]Nanoelectronic Devices Laboratory, École Polytechnique Fédérale de Lausanne, Lausanne, Switzerland

[3] Department of Engineering, University of Cambridge, Cambridge, United Kingdom

***Abstract*—New computation schemes inspired by biological processes can outperform standard von-Neumann architectures in dealing with complex and unstructured tasks. As a new approach, systems of frequency-locked, coupled oscillators are investigated using the phase difference of the signal as the state variable rather than the voltage or current amplitude. As previously shown, these oscillating neural networks can efficiently solve complex tasks such as image recognition. We have built nanometer scale relaxation oscillators based on the insulator-metal transition of VO_2. Coupling these oscillators with an array of tunable resistors offers the perspective of realizing compact oscillator networks. In this work we show experimental coupling of two oscillators. The phase of the two oscillators could be reversibly altered between in-phase and out-of-phase oscillation upon changing the value of the coupling resistor, i.e. by tuning the coupling strength.**

Keywords—Neuromorphic computing, coupled oscillators, VO_2, image recognition, timing, phase, resistive-coupling

I. Introduction

Complex and unstructured problems like image recognition are currently solved on standard Boolean computers with great expense in terms of power dissipation and computing resources, while human brain has proven to be more efficient in dealing with these tasks [1,2]. Therefore, alternative brain-inspired solutions are being researched as hardware accelerators for Neural Networks algorithms [3, 4].

Hopfield networks model the physical phenomena of synchronization of oscillators, that comprise associative memory capabilities [5,6]. Weakly coupled oscillators present time-domain characteristics that can be used for computation: the oscillators lock in frequency, while maintaining a fixed phase difference, determined by the weight of the coupling. Changing the coupling strength, this phase relation can be tuned, advancing the possibility of encoding information in the time-domain.

Using the phase change material VO_2, very compact relaxation oscillators can be fabricated [7]. Previous works obtained stable phase relations in capacitive coupled oscillators [8,9]. In this work two oscillators are coupled with resistive components, and modulation of the phase relations (in-phase and out-of-phase) is demonstrated upon the tuning of the resistive coupling. This kind of network is suitable for performing image recognition tasks [10].

These results could be technologically relevant as they offer the prospective of implementation of the coupling with resistive RAM [11], with a process that respect CMOS compatibility. This would bring to the network the advantage of having reconfigurable weights on chip, allowing online learning of the network.

II. Fabrication

The VO_2 resistors were realized on a 4'' Si wafer over 1μm SiO_2. The VO_2 was deposited with Pulsed Laser Deposition (PLD) for devices 1 and 2, and with Atomic Layer Deposition (ALD) for devices 3 and 4, targeting a thickness of 50 nm. The ALD devices are annealed at 450° for 20 minutes under oxygen flow. Figure 1 shows an ALD-deposited VO_2 film. During the annealing step, grains in the order of 50-80 nm formed in the previously amorphous layer. The film was

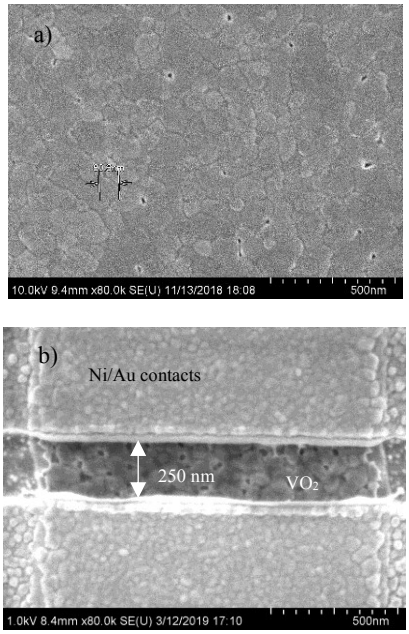

Figure 1: a) SEM image of the VO_2 film on SiO_2. **b)** VO_2 resistor contacted by two metal electrodes (Ni/Au bilayer). Width and length of the devices were varied from 300 nm to several micrometer.

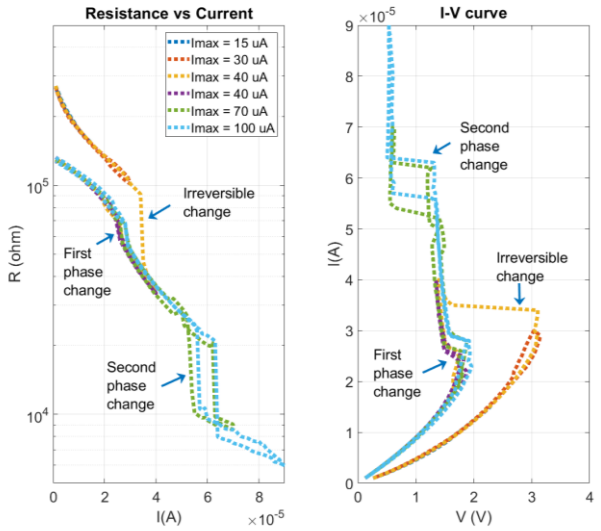

Figure 2: The resistance and I-V characteristics of a VO_2 resistor burning cycle. The current was driven through the device and constantly increased. At around 20μA a first irreversible phase change occurs, that then stabilizes in a minor transition. The real phase change with hysteresis occurs between 60 and 70 μA.

patterned with ICP etching and contacted with Ni/Au electrodes. The test devices are around 300 nm long and 1 μm wide (Figure 1b). The devices were tested in vacuum and contacted with a 16-needle probecard.

First, each device was conditioned with a forming procedure, consisting of consecutive current sweeps with increasing current range. After undergoing a moderate but irreversible change, the device stabilizes showing a reversible phase change. The devices of this batch show two distinct phase changes at different power densities, that we associate with the switching of different grains inside the device (Figure 2).

III. Experimental Results

The basic relaxation-oscillator circuit is depicted in Figure 3. Figure 3 shows the circuit configuration for a single oscillator on the top and for two coupled oscillators on the bottom. The VO_2 resistors were connected to external capacitors and resistors. The series and coupling resistances R_{si} and R_c are implemented with a variable resistor array. The parallel capacitors C_i was implemented with an external component, increasing the time constant of the circuit and therefore obtaining slower oscillations to comply with the maximum sampling frequency of the set-up.

For a single device, the maximum oscillation frequency obtained with the current design was also explored. The oscillation period can be described by the equation [1]:

$$\tau = \tau_r \ln\left(\frac{V_{IN} * H - V_L}{V_{IN} * H - V_H}\right) + \tau_f \ln\left(\frac{V_{IN} * L - V_L}{V_{IN} * L - V_H}\right)$$

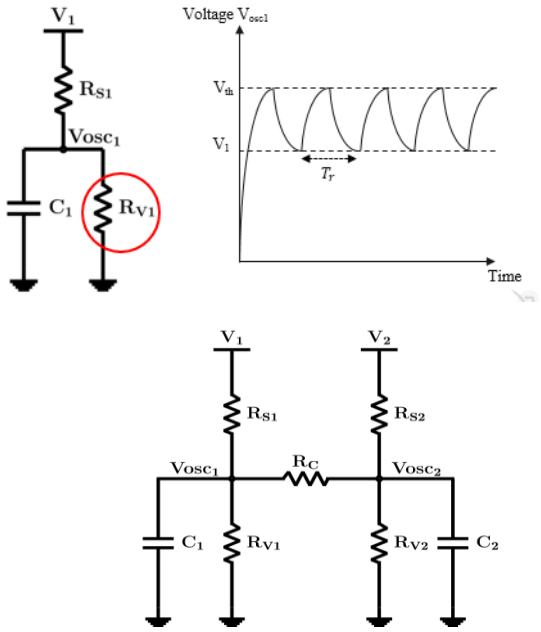

Figure 3: Top: circuit scheme of one relaxation oscillator and corresponding output oscillations.
Bottom: circuit scheme of two relaxation oscillators with resistive coupling.

Where $\tau_{r,f} = C^*(R_s||R_{ins,met})$, with $R_{ins,met}$ being the insulating and metallic values of the VO_2 resistor; H, L = $(R_{ins,met})/(R_{ins,met} + R_s)$; V_L, V_H the voltage thresholds for which the device changes its phase. Varying the external capacitor until the point in which the frequency of the oscillations reached its maximum, we could assess that the maximum oscillation frequency obtained with the current device design is of 10^5Hz. The parasitic capacitance of our circuitry limits the oscillation frequency. Extrapolation of the curve in Figure 4 gives a value of the internal capacitance of around 2nF. With more careful designed circuits we expect that the frequency of oscillation can be increased to 1-10 MHz.

Pairs of coupled oscillators from the PLD and ALD batches were investigated. Two VO_2 switches with equal dimensions were contacted with external probes. The values for the input voltages V_1 and V_2 were chosen to establish stable oscillation conditions for the individual VO_2 oscillators, while the values of the coupling resistors R_c and self-coupling elements R_{si} were tuned to obtain the different phase conditions of the oscillators. The spontaneous oscillations of a first set of coupled VO_2 resonators are shown in Figure 5 (devices 1 and 2 from PLD deposition). An input voltage of 3.2 V was applied to both oscillators, and the chosen values of the self-coupling elements are R_{S1} = 26 kΩ, R_{S2} = 12 kΩ. Setting the coupling resistors R_C = 3 kΩ leads to in-phase oscillations (Δφ=1.06°) whereas R_C = 9 kΩ couples the oscillators out-of-phase (Δφ=179°). The frequencies are 420 Hz for in-phase and 312 Hz for out-of-phase coupling.

For the out-of-phase configuration the shape of the relaxation oscillator presents a double-peak behavior. This is due to the fact that the devices presents quite different resistances and

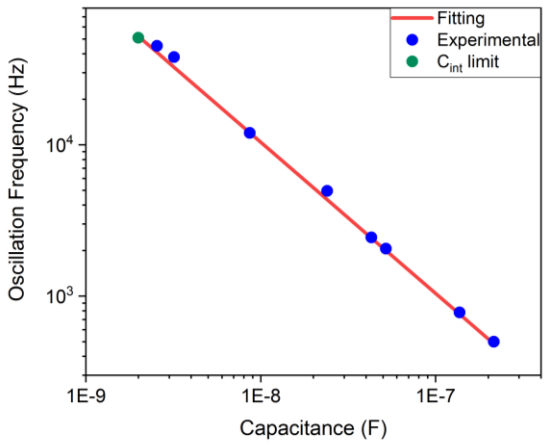

Figure 4: Relation between the oscillation frequency and the external capacitance (experiments fitted with equation 1). The last point shows the value of the internal capacitance of the device, around 2nF.

voltage level values (V_{TH1} = 1.9 V, V_{TL1} = 0.77 V, V_{TH2} = 2.2V, V_{TL2} = 0.67 V for out-of-phase configuration and V_{TH1} = 2 V, V_{TL1} = 0.77V, V_{TH2} = 2.1 V, V_{TL2} = 1 V for in phase configuration, R_{V1H} = 39.4 kΩ and R_{V2H} =23 kΩ for the high impedance state and R_{V1L} = 7.6 kΩ and R_{V2L} = 2.8 kΩ for the low impedance states). The relative difference in resistance value, calculated as $(R_1-R_2)/R_{avarage}$ and averaged between the metallic and insulating state, is of 72%. Due to this difference, a rather strong coupling is required to obtain frequency and phase locking of the oscillators. With such a strong coupling the exponential rise in voltage of the oscillator in the high-impedance state is influenced by the phase change of the second oscillator, from which the distorted oscillation shape arises.

Circuit simulation were performed to match the experimental results. The VO_2 device was modelled with the equivalent circuit described in [12]. Systematic simulations show that in a network of two coupled oscillators only 2 stable phase conditions exist: either the in-phase or the out-of-phase coupling. Scanning the coupling-resistance parameter space, every intermediate phase relation is converging within 2-3 oscillations to either in-phase or out-of-phase coupling. The simulation moreover shows that for different devices the out-of-phase configuration is the preferred one, while identical devices are more likely to couple in the in-phase configuration.

Coupling of more than two devices is for now limited by the variability of the VO_2 switches. Improvements of the film quality has already been achieved with the ALD- deposited films, that reduce the device variability allowing different coupling schemes.

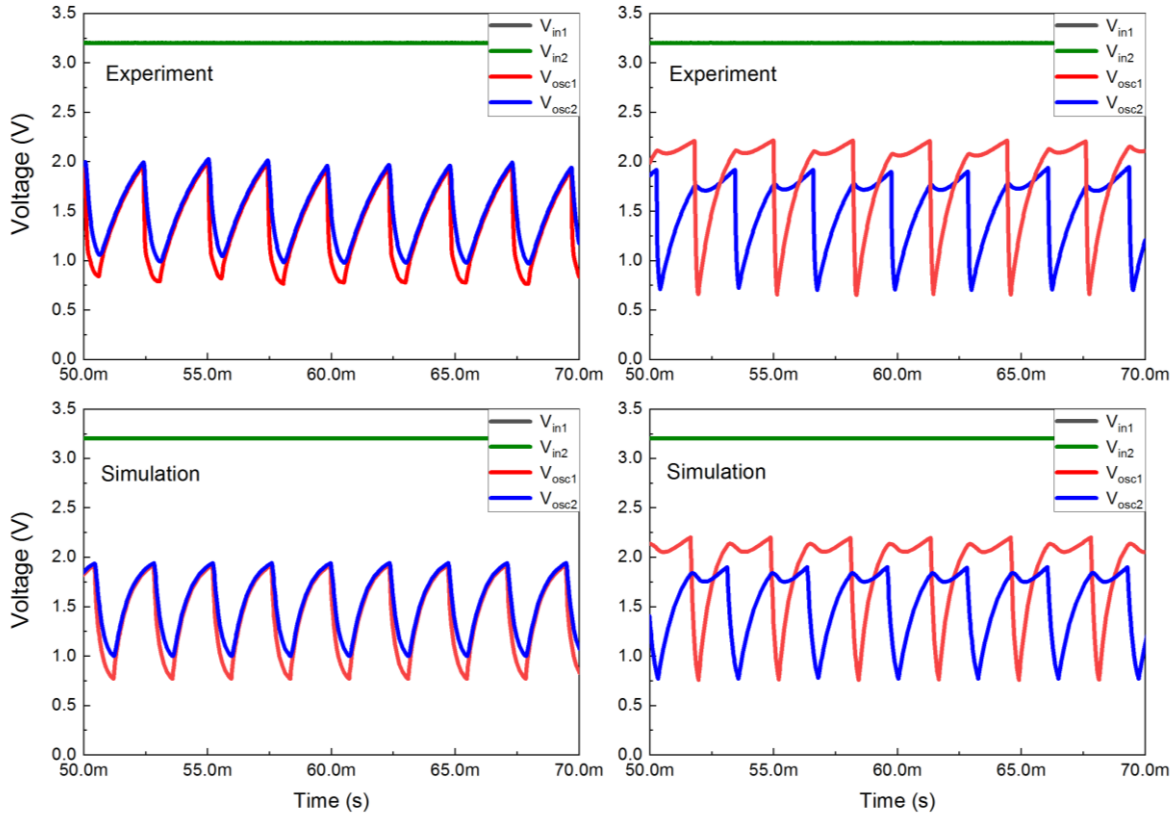

Figure 5: Measured voltage oscillations of coupled VO_2 resonators. Changing the value of the coupling resistance, different phase configurations are achieved. R_C=3k kΩ results in in-phase coupling (left), R_C=9 kΩ in out-of-phase coupling (right). Circuit parameters: V_1=V_2=3.2V, R_{S1}=26 kΩ , R_{S2}=12 kΩ , C_1 = C_2 = 150 nF.
Bottom: circuit simulation matching the experimental results.

In Figure 6 the in-phase and out-of-phase coupling of ALD-deposited devices 3 and 4 is shown.

In this case it was necessary to change also the self-coupling elements to bias the circuit in the oscillation condition. Details about the circuit parameters are given in Figure 6. For the ALD prepared films, the devices present similar voltage thresholds for the switching and similar resistances parameters ($R_{ins3,4}$ = 37-33.5 kΩ, $R_{met3,4}$= 6-4.7 kΩ). The variation was greatly improved. The relative difference of the resistances was calculated to be around 15%. Therefore, a less strong coupling is required to lock the oscillators in frequency. Though the coupling resistances were much larger than in the previous example, the double-peak behavior is still observed, but appears to be less pronounced.

The in-phase configuration of this pair of oscillators shows an interesting feature: the first device changes to the metallic state and the output voltage V_{osc3} stays fixed at a value slightly larger than the threshold voltage $V_{TL2,}$ necessary to trigger the metal to insulator transition. The threshold is reached only when the first device also changes his phase, becoming metallic and lowering the voltage partition across the VO_2 resistors. The minimum peaks of the two devices are aligned, as shown in the enlargement in Figure 7: the metal to insulator transition happens in-phase for the coupled oscillators.

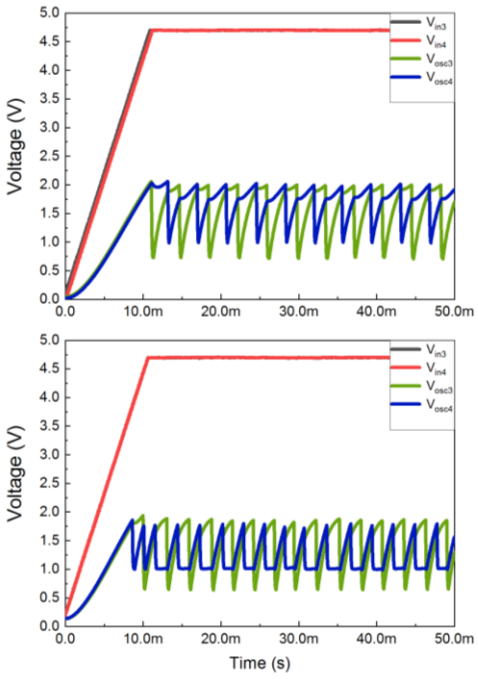

Figure 6: Measured voltage oscillations of coupled Devices 3 and 4. Top: in-phase oscillations. Circuit parameters: V_1=V_2=4.7V, C_1=C_2=150nF, R_{S1}=30 kΩ, R_{S2}=33 kΩ, Rc=29 kΩ. Bottom: out-of-phase oscillations. Circuit parameters: V_1=V_2=4.7V, C_1=C_2=150nF, R_{S1}=33 kΩ, R_{S2}=36 kΩ, Rc=27 kΩ.

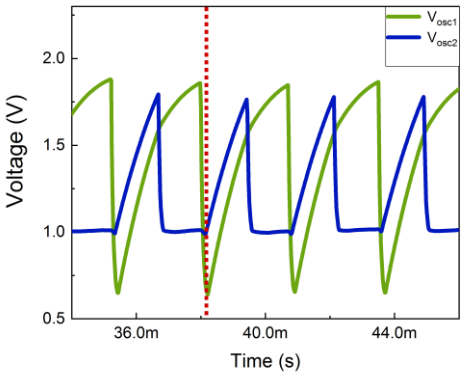

Figure 7: Enlargement of the in-phase oscillations obtained for Dev 3 and 4. The minimums of the two oscillators is perfectly aligned, therefore giving in-phase coupling of the devices.

IV. CONCLUSION

Highly scalable electrical relaxation-oscillators can be built using VO_2 metal-insulator switches. In this paper we showed through experimental results frequency and phase-locking of a double oscillator system. With experiments and circuits simulations we achieved control of the phase relation between the two oscillators using variable resistors as coupling elements. The ability to perform coupled oscillation is strongly constrained when the resistances of the individual oscillator diverge. Ultimately, improvements of the VO_2 film quality are required to obtain more similar oscillator and therefore limit the distortion introduced by a rather strong coupling. This experimental work opens the perspective of employing this technology for dedicated hardware for neuromorphic computing, in particular for application for convolutional neural networks.

ACKNOWLEDGMENT

This work has been supported by the HORIZON 2020 PHASE-CHANGE SWITCH Project (Grant. No. 737109).

REFERENCES

[1] C. D. Schuman *et al.*, [online] CoRR, abs/1705.06963, 2017.
[2] J. Misra and I. Saha," *Neurocomputing*, 74, 239–255, 2010.
[3] D. Kuzum *et al*., *Nanotechnology*, 24,38, 2013.
[4] G. Indiveri and S. C. Liu, *Proc. IEEE*, 103, 1379–1397, 2015.
[5] Izhikevich, *Neural Networks*, 5255, 1–30, 2000.
[6] Endo, T. and Takeyama, *Electron. Comm. Jpn. Pt. III*, 75, 51-59, 1992.
[7] N. Shukla et al., *Sci. Rep.* 4, doi:10.1038/srep04964 (2014).
[8] A. Parihar *et al., J. Appl. Phys.*, vol. 117, no. 5, 2015.
[9] V. V Perminov, V *et al., J. Phys. Conf. Ser.*, 929, 12045, 2017
[10] E. Corti et al., , Proc. IEEE ICRC, 2018, DOI: 10.1109/ICRC.2018.8638626
[11] G. W. Burr *et al., Advances in Physics: X*, 2, 89-124, 2016.
[12] P. Maffezzoni *et al, IEEE Trans. Circuits Syst.*, 62, 2207–2215, 2015.